Hindawi
Mathematical Problems in Engineering
Volume 2021, Article ID 8024879, 13 pages
https://doi.org/10.1155/2021/8024879

Research Article

Revisited on the Free Vibration of a Cantilever Beam with an Asymmetrically Attached Tip Mass

Xiangsheng Lei,[1] Yanfeng Wang,[1] Xinghua Wang,[1] Gang Lin ,[2] and Shihong Shi[2]

[1]*Research Center of Grid Planning, Guangdong Power Grid Corporation, Guangzhou 510080, China*
[2]*China Energy Engineering Group Guangdong Electric Power Design Institute Co., Ltd., Guangzhou 510663, China*

Correspondence should be addressed to Gang Lin; lingang@gedi.com.cn

Received 28 July 2021; Accepted 1 September 2021; Published 13 September 2021

Academic Editor: Francesco Pellicano

Cantilever with an asymmetrically attached tip mass arises in many engineering applications. Both the traditional method of separation of variables and the method of Laplace transform are employed in the present paper to solve the eigenvalue problem of the free vibration of such structures, and the effect of the eccentric distance along the vertical direction and the length direction of the tip mass is considered here. For the traditional method of separation of variables, tip mass only affects to the boundary conditions, and the eigenvalue problem of the free vibration is solved based on the nonhomogeneous boundary conditions. For the method of Laplace transform, the effect of the tip mass is introduced in the governing equation with the Dirac function, and the eigenvalue problem then can be solved through Laplace transform with homogeneous boundary conditions. The computed results with these two methods are compared well with the numerical solution obtained by finite element method and approximate analytical solutions, and the effect of tip mass dimensions on the natural frequencies and corresponding mode shapes is also given.

1. Introduction

In engineering practices, the problem of a beam carrying a concentrated mass at its end or middle may arise. For instance, offshore wind turbines [1], mast antenna structures, wind tunnel stings carrying an airplane or a missile model, large aspect ratio wings carrying heavy tip tanks, or launch vehicles with payload at the tip [2], and all these structures can be modeled as a beam carrying a concentrated mass at its end or middle. In these applications, the concept of an ideal concentrated mass or moment of initial is often not applicable, as the attachment point does not coincide with the center of gravity of the mass. Researchers had paid more attention to the free vibrations of this subject. Generally, two approaches are adopted to solve this free vibration problem: the traditional method of separation of variables (MSV) and the method of Laplace transform (MLT).

The most widely used approach solves the homogeneous partial differential equation that describes the free vibration with separation of variables to yield a pair of ordinary differential equations, and then, with the requirement of the nontrivial solution of the linear equations based on the introduction of nonhomogeneous boundary conditions, frequency equation and mode shape can be obtained consequently. This approach is described as the traditional method of separation of variables (MSV), as it mainly depends on the nonhomogeneous boundary conditions. Bhat et al. gave the natural frequencies of a uniform cantilever with a tip mass slender in the axial direction based on the perturbation procedure, in which rotary inertial is also considered [2, 3]. Recently, Mousavi Lajimi and Heppler corrected some errors in Bhat and Wagner's paper [4], and Bhat responded back with a closure [5]. Wang et al. also proposed an improved analytical method of calculations for natural frequencies and mode shapes of a uniform cantilever beam carrying a tip mass under base excitation [6]. It is noted that they did not consider the effect of the eccentric distance along the vertical direction of the tip mass [6]. Anderson pointed out that due to the importance in airplane and missile design, it is of interest to consider the problem

that the centroid of the tip mass does not coincide with its point of attachment to the beam which offsets an arbitrary distance perpendicular to the extended neutral axis of the beam [7]. Anderson also showed that the longitudinal and transverse deflections in the beam become coupled through the boundary conditions because of the presence of the asymmetrically attached tip mass. Natural frequencies and mode shapes of a cantilever beam with a base excitation and asymmetric tip mass were given by To [8]. Many other researchers also used this approach to investigate the vibrations of a cantilever with concentrate mass under different boundary conditions [9–16].

The other approach introduces the tip mass by means of a Dirac function to make the constant density beam a variable density one [17], and the governing partial differential equations can be solved based on the method of separation of variables and the Laplace transform under homogeneous boundary conditions. This approach is described as the method of Laplace transform (MLT), as it mainly depends on the Laplace transform to solve the differential equation. The advantage of this method is that if there are many concentrated mass located along the length direction of the beam, it is unnecessary to solve the problem by considering many individual spans separated by these concentrated masses. Chen adopted this method to solve the free vibration and forced vibration problem of a simply supported beam with a middle concentrated mass [18], and the concentrated mass is just considered as a point mass. When the dimensions of the concentrated mass are too big to be ignored, the problem of how to consider the tip mass effect arises. Goel investigated vibrations of a beam carrying a concentrated mass that one end of the beam is free and the other end is hinged by a rotational spring of constant stiffness with this method [19, 20]. Liu and Huang [21] and Chang [22] investigated the free vibration and forced vibration of a beam carrying a concentrated mass at the beam tip and another concentrated mass at an intermediate point, respectively. Park et al. investigated a Bernoulli–Euler beam fixed on a moving cart and carrying a concentrated mass attached to an arbitrary position along the beam length [23].

It should be pointed out that, most of the investigations either ignore the rotational inertia of the tip mass or ignore the eccentric effect of the tip mass, and in some situations, these effects cannot be neglected. Therefore, the purpose of this paper is to conduct the free vibration analysis of the cantilever with an asymmetrically attached tip mass with both the conventional method of separation of variables and method of Laplace transform and to clarify the introduction of concentrate force and moment in the method of Laplace transform.

2. Mathematical Model

A schematic sketch of the cantilever is shown in Figure 1, and L_b and L_m denote the length of the beam and the tip mass, respectively, e_h and $e_L = L_m/2$ are the distance between point of attachment A and the center of gravity of the tip mass C along the vertical and length direction, respectively, and h_b and h_m denote the heights of the beam and the tip mass, respectively. The tip mass and the beam are assumed to have the same width b. The total mass of the tip mass is m.

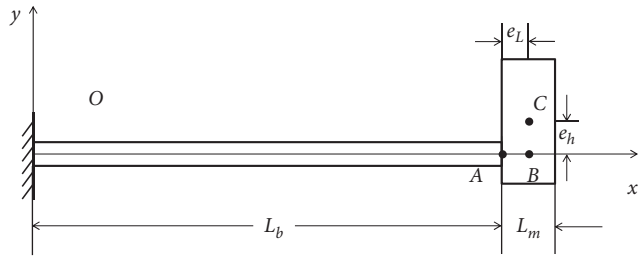

Figure 1: Schematic of a cantilever with an asymmetrical tip mass.

2.1. Method of Separation of Variables. In this section, the homogeneous partial differential equation which describes the free vibration of the cantilever beam is solved by the MSV. For the method of separation of variables, the effect of tip mass to the free vibration is introduced by the nonhomogeneous boundary conditions [24].

Hamilton's principle is applied here to obtain the governing equations of the system:

$$\int_{t_0}^{t_1} \delta(T - V)\mathrm{d}t = 0, \tag{1}$$

where T and V denote the kinetic and potential energies, respectively, δ is the variation operator, and t_0 and t_1 are arbitrary times. The potential energy is given by

$$V = \frac{1}{2}\int_0^{L_b} EIw''\,\mathrm{d}x. \tag{2}$$

The total kinetic energy consists of the contributions from the beam T_b and the tip mass T_m:

$$T = T_b + T_m, \tag{3}$$

$$T_b = \frac{1}{2}\rho_b A\int_0^{L_b} \dot{w}^2\mathrm{d}x, \tag{4}$$

$$T_m = \int_{L_b}^{L_b+L_m}\int_{e_h-(h_m/2)}^{e_h+(h_m/2)} \frac{1}{2}\rho_m b_m v_m^2\,\mathrm{d}x\mathrm{d}y, \tag{5}$$

where the velocity of the representative elemental volume v_m is given by

$$v_m = \sqrt{\left(\dot{w}_L' y\right)^2 + \left(\dot{w}_L + \dot{w}_L'(x - L_b)\right)^2}. \tag{6}$$

In the above formulations, primes and dots denote differentiation with regard to coordinate x and time t, respectively, E denotes Young's modulus for the beam material, A and I are constant cross-section area and moment of inertia, respectively, and ρ_b and ρ_m denote density of the beam and tip mass material, respectively. The flexural deflection of the beam is denoted by w, and w_L is the deflection of the beam at $x = L_b$.

Substituting equations (2)–(6) into equation (1) and carrying out the necessary variations, the following equation for undamped free vibration under small deflection is obtained:

$$EIw^{'''\prime} + \rho_b A\ddot{w} = 0. \tag{7}$$

The corresponding boundary conditions at the fixed end $x = 0$ are

$$w(0,t) = 0, \tag{8}$$

$$w'(0,t) = 0, \tag{9}$$

and at the tip $x = L_b$ are

$$EIw^{'''}(L_b,t) - m\ddot{w}(L_b,t) - me_L\ddot{w}'(L_b,t) = 0, \tag{10}$$

$$EIw''(L_b,t) + \left(J_m + m\left(e_L^2 + e_h^2\right)\right)\ddot{w}'(L_b,t) + me_L\ddot{w}(L_b,t) = 0, \tag{11}$$

where $I = (bh_b^3/12)$ and $J_m = (m(L_m^2 + h_m^2)/12)$ are the moment of inertia of the beam cross-section and the tip mass, respectively. These vibration equation and corresponding boundary conditions are the same as in [7].

For undamped free vibration of natural frequency ω, one may assume that

$$w(x,t) = \phi(x)\eta(t). \tag{12}$$

Substituting equation (12) into equation (7), we have

$$EI\phi''''(x)\eta(t) + \rho_b A\phi(x)\ddot{\eta}(t) = 0, \tag{13}$$

or

$$\phi^{'''\prime} - \frac{\rho_b A\omega^2}{EI}\phi = 0, \tag{14}$$

$$\ddot{\eta} + \omega^2\eta = 0. \tag{15}$$

The general solution for equation (14) is given by

$$\phi(x) = A\sin\lambda x + B\cos\lambda x + C\sinh\lambda x + D\cosh\lambda x, \tag{16}$$

where A, B, C, and D are constants to be determined by boundary conditions (8)–(11) and $\lambda^4 = (\rho_b A\omega^2/EI)$.

Substituting equation (16) into boundary conditions (8)–(11), we have

$$\phi(0) = 0, \tag{17}$$

$$\phi'(0) = 0, \tag{18}$$

$$\phi^{'''}(L_b) + \frac{me_L\omega^2}{EI}\phi'(L_b) + \frac{m\omega^2}{EI}\phi(L_b) = 0, \tag{19}$$

$$\phi''(L_b) - \frac{\left(J_m + m\left(e_L^2 + e_h^2\right)\right)\omega^2}{EI}\phi'(L_b) - \frac{me_L\omega^2}{EI}\phi(L_b) = 0. \tag{20}$$

Considering equation (17) and (18), we have

$$\phi(x) = A(\sin\lambda x - \sinh\lambda x) + B(\cos\lambda x - \cosh\lambda x). \tag{21}$$

Substituting equation (21) into boundary conditions (19) and (20), then they can be written in matrix form:

$$\begin{bmatrix} \Omega_{11} & \Omega_{12} \\ \Omega_{21} & \Omega_{22} \end{bmatrix}\begin{Bmatrix} A \\ B \end{Bmatrix} = \begin{pmatrix} 0 \\ 0 \end{pmatrix}, \tag{22}$$

where $\Omega_{11} = -\lambda^3(\cos\lambda L_b + \cosh\lambda L_b) + c_2\lambda(\cos\lambda L_b - \cosh\lambda L_b) + c_1(\sin\lambda L_b - \sinh\lambda L_b)$, $\Omega_{12} = \lambda^3(\sin\lambda L_b - \sinh\lambda L_b) - c_2\lambda(\sin\lambda L_b + \sinh\lambda L_b) + c_1(\cos\lambda L_b - \cosh\lambda L_b)$, $\Omega_{21} = -\lambda^2(\sin\lambda L_b + \sinh\lambda L_b) - c_3\lambda(\cos\lambda L_b - \cosh\lambda L_b) - c_2(\sin\lambda L_b - \sinh\lambda L_b)$, and $\Omega_{22} = -\lambda^2(\cos\lambda L_b + \cosh\lambda L_b) + c_3\lambda(\sin\lambda L_b + \sinh\lambda L_b) - c_2(\cos\lambda L_b - \cosh\lambda L_b)$ and $c_1 = (m\omega^2/EI)$, $c_2 = (me_L\omega^2/EI)$, and $c_3 = ((J_m + m(e_L^2 + e_h^2))\omega^2/EI)$.

Based on the untrivial solution condition of equation (22), the frequency equation can be obtained, in principle, by setting the coefficient determinant to zero:

$$\Omega_{11}\Omega_{22} - \Omega_{12}\Omega_{21} = 0. \tag{23}$$

The roots of equation (23) gives the natural frequencies $\omega_i (i = 1, 2, 3, \ldots)$; then, by substituting ω_i into equations (22) and (21), one can obtain the constant A and B and the corresponding mode shape $\phi_i(x)$. It is also noted that the natural frequencies were determined by a trial and error method based on interpolation and the bisection approach with MATLAB. The iterative computations were terminated when the value of ω_i reached the relative error of 10^{-5}.

2.2. Method of Laplace Transform. In order to describe the effect of the asymmetrically attached tip mass, the Dirac δ-function is used in the differential equation which is defined by the following equation:

$$\int_{-\infty}^{+\infty}\delta(x - L_b)\mathrm{d}x = 1. \tag{24}$$

The effect of the tip mass is introduced by the concentrated equivalent force F_m and moment M_m at the attachment point A of the beam, and then, the undamped free vibration equation under small deflection is

$$EIw^{'\prime'''} + \rho_b A\ddot{w} + F_m\delta(x - L_b) + M_m\delta'(x - L_b) = 0, \tag{25}$$

where

$$F_m = m\ddot{w}(L_b,t) + me_L\ddot{w}'(L_b,t),$$
$$M_m = -me_L\ddot{w}(L_b,t) - \left(J_m + m\left(e_L^2 + e_h^2\right)\right)\ddot{w}'(L_b,t). \tag{26}$$

With this treatment, the boundary conditions become homogeneous, which is given by

$$w(0,t) = 0, \tag{27}$$

$$w'(0,t) = 0, \tag{28}$$

$$w'''(L_b,t) = 0, \tag{29}$$

$$w''(L_b,t) = 0. \tag{30}$$

Based on separation of variables, for undamped free vibration of natural frequency ω, one may assume that

$$w(x,t) = \phi(x)\sin\ \omega t. \tag{31}$$

Substituting equation (31) into equations (25)–(30), we have

$$\phi'''' - \lambda^4\phi - \delta(x-L_b)\left(c_1\phi(L_b) + c_2\phi'(L_b)\right) + \delta'(x-L_b)\left(c_2\phi(L_b) + c_3\phi'(L_b)\right) = 0, \tag{32}$$

$$\phi(0) = 0, \tag{33}$$

$$\phi'(0) = 0, \tag{34}$$

$$\phi'''(L_b) = 0, \tag{35}$$

$$\phi''(L_b) = 0, \tag{36}$$

where $\lambda^4 = (\rho_b A\omega^2/EI)$ and $c_1 = (m\omega^2/EI), c_2 = (me_L\omega^2/EI)$, and $c_3 = ((J_m + m(e_L^2 + e_h^2))\omega^2/EI)$.

Equations (32)–(36) define an eigenvalue problem, and the solution can be obtained by the Laplace transform method. Let the transformed function of ϕ be denoted by $\overline{\phi}$, and the definition of the Laplace transform is given by

$$\overline{\phi}(s) = \mathfrak{L}(\phi(x)) = \int_{-\infty}^{+\infty}\phi(x)e^{-sx}\mathrm{d}x. \tag{37}$$

Then, we have

$$\mathfrak{L}(\phi'''') = s^4\overline{\phi} - \phi'''(0) - s\phi''(0) - s^2\phi'(0) - s^3\phi(0), \tag{38}$$

$$\mathfrak{L}\left(-\lambda^4\phi\right) = -\lambda^4\overline{\phi}. \tag{39}$$

Considering the boundary conditions (33) and (34), we have

$$\mathfrak{L}(\phi'''') = s^4\overline{\phi} - \phi'''(0) - s\phi''(0). \tag{40}$$

The shifting property of the Dirac δ-function is given by

$$\int_{-\infty}^{+\infty}\phi(x)\delta(x-x_0)\mathrm{d}x = \phi(x_0), \tag{41}$$

and then, we have

$$\mathfrak{L}(-c_1\delta(x-L_b)\phi(L_b)) = -c_1\phi(L_b)\int_{-\infty}^{+\infty}\delta(x-L_b)e^{-sx}\mathrm{d}x = -c_1\phi(L_b)(e^{-sx})|_{x=L_b} = -c_1\phi(L_b)e^{-sL_b}, \tag{42}$$

$$\mathfrak{L}(-c_2\delta(x-L_b)\phi'(L_b)) = -c_2\phi'(L_b)\int_{-\infty}^{+\infty}\delta(x-L_b)e^{-sx}\mathrm{d}x = -c_2\phi'(L_b)(e^{-sx})|_{x=L_b} = -c_2\phi'(L_b)e^{-sL_b}. \tag{43}$$

The definition of the derivatives of the Dirac δ-function is given by

$$\int_{-\infty}^{+\infty}\phi(x)\delta'(x-x_0)\mathrm{d}x = -\phi'(x_0), \tag{44}$$

and then, we have

$$\mathfrak{L}(c_2\delta'(x-L_b)\phi(L_b)) = c_2\phi(L_b)\int_{-\infty}^{+\infty}\delta'(x-L_b)e^{-sx}\mathrm{d}x = -c_2\phi(L_b)(e^{-sx})'|_{x=L_b} = -c_2\phi(L_b)se^{-sL_b}, \tag{45}$$

$$\mathfrak{L}(c_3\delta'(x-L_b)\phi'(L_b)) = c_3\phi'(L_b)\int_{-\infty}^{+\infty}\delta'(x-L_b)e^{-sx}\mathrm{d}x = -c_3\phi'(L_b)(e^{-sx})'|_{x=L_b} = -c_3\phi'(L_b)se^{-sL_b}. \tag{46}$$

Substituting equations (39)–(46) into equation (32), then we have

$$\overline{\phi} = \frac{s}{s^4 - \lambda^4}\phi''(0) + \frac{1}{s^4 - \lambda^4}\phi'''(0) + \left(c_1\phi(L_b) + c_2\phi'(L_b)\right)\frac{e^{-sL_b}}{s^4 - \lambda^4} - \left(c_2\phi(L_b) + c_3\phi'(L_b)\right)\frac{se^{-sL_b}}{s^4 - \lambda^4}. \tag{47}$$

Then, the inverse Laplace transform is defined by

$$\phi(x) = \mathfrak{L}^{-1}\left(\overline{\phi}(s)\right) = \frac{1}{2\pi j}\int_{-j\infty}^{+j\infty}\overline{\phi}(s)e^{-sx}\mathrm{d}x. \tag{48}$$

Through the inverse Laplace transform, we have

$$\mathfrak{L}^{-1}\left(\frac{s}{s^4 - \lambda^4}\right) = \frac{1}{2\lambda^2}(\cosh\lambda x - \cos\lambda x), \tag{49}$$

$$\mathfrak{L}^{-1}\left(\frac{1}{s^4 - \lambda^4}\right) = \frac{1}{2\lambda^3}(sinh\lambda x - \sin\lambda x), \tag{50}$$

$$\mathfrak{L}^{-1}\left(\frac{e^{-sL_b}}{s^4 - \lambda^4}\right) = \frac{1}{2\lambda^3}\left(\sinh\lambda(x - L_b) - \sin\lambda(x - L_b)\right)H(x - L_b), \tag{51}$$

$$\mathfrak{L}^{-1}\left(\frac{se^{-sL_b}}{s^4 - \lambda^4}\right) = \frac{1}{2\lambda^2}\left(\cosh\lambda(x - L_b) - \cos\lambda(x - L_b)\right)H(x - L_b), \tag{52}$$

where $H(x - L_b)$ is the unit step function at $x = L_b$.

Substituting equations (49)–(52) into equation (47), then we have the general solution of equation (32) as follows:

$$\begin{aligned}\phi(x) = {} & \frac{\phi''(0)}{2\lambda^2}(\cosh\lambda x - \cos\lambda x) + \frac{\phi'''(0)}{2\lambda^3}(\sinh\lambda x - \sin\lambda x) \\ & + \frac{c_1\phi(L_b) + c_2\phi'(L_b)}{2\lambda^3}\left(\sinh\lambda(x - L_b) - \sin\lambda(x - L_b)\right)H(x - L_b) \\ & - \frac{c_2\phi(L_b) + c_3\phi'(L_b)}{2\lambda^2}\left(\cosh\lambda(x - L_b) - \cos\lambda(x - L_b)\right)H(x - L_b),\end{aligned} \tag{53}$$

$$\begin{aligned}\phi'(x) = {} & \frac{\phi''(0)}{2\lambda}(\sinh\lambda x + \sin\lambda x) + \frac{\phi'''(0)}{2\lambda^2}(\cosh\lambda x - \cos\lambda x) \\ & + \frac{c_1\phi(L_b) + c_2\phi'(L_b)}{2\lambda^2}\left(\cosh\lambda(x - L_b) - \cos\lambda(x - L_b)\right)H(x - L_b) \\ & - \frac{c_2\phi(L_b) + c_3\phi'(L_b)}{2\lambda}\left(\sinh\lambda(x - L_b) + \sin\lambda(x - L_b)\right)H(x - L_b),\end{aligned} \tag{54}$$

$$\begin{aligned}\phi''(x) = {} & \frac{\phi''(0)}{2}(\cosh\lambda x + \cos\lambda x) + \frac{\phi'''(0)}{2\lambda}(\sinh\lambda x + \sin\lambda x) \\ & + \frac{c_1\phi(L_b) + c_2\phi'(L_b)}{2\lambda}\left(\sinh\lambda(x - L_b) + \sin\lambda(x - L_b)\right)H(x - L_b) \\ & - \frac{c_2\phi(L_b) + c_3\phi'(L_b)}{2}\left(\cosh\lambda(x - L_b) + \cos\lambda(x - L_b)\right)H(x - L_b),\end{aligned} \tag{55}$$

$$\begin{aligned}\phi'''(x) = {} & \frac{\lambda\phi''(0)}{2}(\sinh\lambda x - \sin\lambda x) + \frac{\phi'''(0)}{2}(\cosh\lambda x + \cos\lambda x) \\ & + \frac{c_1\phi(L_b) + c_2\phi'(L_b)}{2}(\cosh\lambda(x-L_b) + \cos\lambda(x-L_b))H(x-L_b) \\ & - \frac{\lambda(c_2\phi(L_b) + c_3\phi'(L_b))}{2}(\sinh\lambda(x-L_b) - \sin\lambda(x-L_b))H(x-L_b).\end{aligned} \tag{56}$$

It is noted that items with $\delta(x-L_b)$, $\delta'(x-L_b)$, and $\delta''(x-L_b)$ are ignored in equations (54)–(56), as they will not affect the final results.

Substituting equations (55) and (56) into boundary conditions' equations (35) and (36), then the constants $\phi''(0)$ and $\phi'''(0)$ can be obtained by

$$\begin{aligned}\phi''(0) &= \frac{\lambda b_1(\cosh\lambda L_b + \cos\lambda L_b) + b_2(\sinh\lambda L_b + \sin\lambda L_b)}{\lambda(1 + \cos\lambda L_b\cosh\lambda L_b)}, \\ \phi'''(0) &= \frac{\lambda b_1(\sin\lambda L_b - \sinh\lambda L_b) - b_2(\cosh\lambda L_b + \cos\lambda L_b)}{1 + \cos\lambda L_b\cosh\lambda L_b},\end{aligned} \tag{57}$$

where $b_1 = c_2\phi(L_b) + c_3\phi'(L_b)$ and $b_2 = c_1\phi(L_b) + c_2\phi'(L_b)$.

Substituting equation (57) into equations (53) and (54), let $x = L_b$, and the following two equations are obtained:

$$\begin{bmatrix}\Lambda_{11} & \Lambda_{12} \\ \Lambda_{21} & \Lambda_{22}\end{bmatrix}\begin{Bmatrix}\phi(L_b) \\ \phi'(L_b)\end{Bmatrix} = \begin{pmatrix}0 \\ 0\end{pmatrix}, \tag{58}$$

where $\Lambda_{11} = \lambda^3(1 + \cos\lambda L_b\cosh\lambda L_b) + c_1(\cos\lambda L_b\sinh\lambda L_b - \cosh\lambda L_b\sin\lambda L_b) - c_2\lambda\sin\lambda L_b\sinh\lambda L_b$, $\Lambda_{12} = c_2(\sinh\lambda L_b\cos\lambda L_b - \cosh\lambda L_b\sin\lambda L_b) - c_3\lambda\sinh\lambda L_b\sin\lambda L_b$, $\Lambda_{21} = c_2\lambda(\cos\lambda L_b\sinh\lambda L_b + \cosh\lambda L_b\sin\lambda L_b) + c_1\sin\lambda L_b\sinh\lambda L_b$, and $\Lambda_{22} = c_3\lambda(\cos\lambda L_b\sinh\lambda L_b + \cosh\lambda L_b\sin\lambda L_b) + c_2\sin\lambda L_b\sinh\lambda L_b - \lambda^2(1 + \cos\lambda L_b\cosh\lambda L_b)$.

Based on the untrivial solution condition of equation (58), the frequency equation can be obtained, in principle, by setting the coefficient determinant to zero:

$$\Lambda_{11}\Lambda_{22} - \Lambda_{12}\Lambda_{21} = 0. \tag{59}$$

The roots of equation (59) gives the natural frequencies $\omega_i\,(i = 1, 2, 3, \ldots)$; then, by substituting ω_i into equations (53) and (58), one can obtain the constant A and B and the corresponding mode shape $\phi_i(x)$.

3. Numerical Results

In this section, numerical results obtained by ANSYS simulation and analytical solution with the present method of separation of variables and the method of Laplace transform are given and compared for different cantilevers. The effect of several key parameters on the natural frequencies and mode shapes is also presented.

3.1. Verification of the Present Methods. ANSYS is used here to determine the natural frequency and mode shape, and the obtained numerical results are considered as the benchmark solution. The cantilever is modeled as a three dimensional structure and meshed with SOLID186 element. The convergence test is performed in advance to make sure that the numerical solution can be treated as the benchmark solution.

The approximate analytical solution of the first-order natural frequency of a cantilever with the tip mass is given by

$$f_1^{\text{apr}} = \frac{1}{2\pi}\sqrt{\frac{3EI/L_b^3}{(33/140)\rho_b AL_b + m}}. \tag{60}$$

The geometry and physical parameters used in the computation are given in Table 1, and three beam structures with different length L_b are investigated. The first three natural frequencies of different beam structures with different methods are given in Table 2.

The approximate analytical solution of the first-order natural frequency of the three cantilevers is 15.960 Hz, 8.903 Hz, and 5.825 Hz, respectively. It can be seen that, for all the other five methods, the first-order natural frequency results compare well with the approximate analytical solution, as the inertial effect does not play an important role in the first-order free vibration. For the second- and third-order natural frequencies, results with the present MSV and MLT are the same and in good agreement with the ANSYS solution. At the same time, the inertial effect plays a very important role in higher-order natural frequencies for the cantilever with an asymmetrically attached tip mass, and the inertial effect makes the structure more flexible. If inertial effect is ignored, the higher-order natural frequencies can be unconceivable large. It also can be seen that, although inertial effect is taken into consideration, the eccentric effect is also nonignorable. For the 100 mm length cantilever, the second- and third-order natural frequencies are 154 Hz and 579 Hz, respectively. If the inertial effect is neglected, the natural frequencies increase to 322 Hz and 1035 Hz, respectively, and even if we consider the inertial effect, but neglect the eccentricity of the tip mass, the natural frequencies are still as large as 201 Hz and 617 Hz, respectively, which are much larger than those of 154 Hz and 579 Hz, respectively. The comparisons of the first three mode shapes with different methods for different beams are given in Figures 2–4 , and the mode shapes are normalized by the tip displacement.

It can be seen from Figures 2–4 that the present results with both the method of separation of variables (MSV) and method of Laplace transform (MLT) compare well with ANSYS results, while both results without eccentric effect and without inertia effect have an obvious different with the ANSYS results. It is also noted that both natural frequencies

Table 1: Geometry and physical parameters for the beam structure.

Parameter	Value
L_b	100, 150, and 200 mm
L_m	15 mm
h_b	1 mm
h_m	30 mm
b	10 mm
e_h	10 mm
e_L	7.5 mm
ρ_m	8900 kg/m^3
ρ_b	7800 kg/m^3
E	210 GPa

Table 2: Comparisons of the first three natural frequencies of different beam structures with different methods.

	$L_b = 100$ mm			$L_b = 150$ mm			$L_b = 200$ mm		
	f_1 (Hz)	f_2 (Hz)	f_3 (Hz)	f_1 (Hz)	f_2 (Hz)	f_3 (Hz)	f_1 (Hz)	f_2 (Hz)	f_3 (Hz)
Results from equation (59)	15.960	—	—	8.903	—	—	5.825	—	—
ANSYS	15.849	153.42	576.04	8.9144	103.98	286.84	5.8490	72.251	186.85
Present MSV	15.780	153.98	579.12	8.8868	103.99	288.02	5.8350	72.148	187.36
Present MLT	15.780	153.98	579.12	8.8868	103.99	288.02	5.8350	72.148	187.36
Results without eccentric effect	15.925	200.75	616.90	8.9241	123.41	326.90	5.8344	79.434	217.52
Results without inertial effect	15.960	322.03	1035.0	8.9021	150.85	483.08	5.8246	87.373	278.82

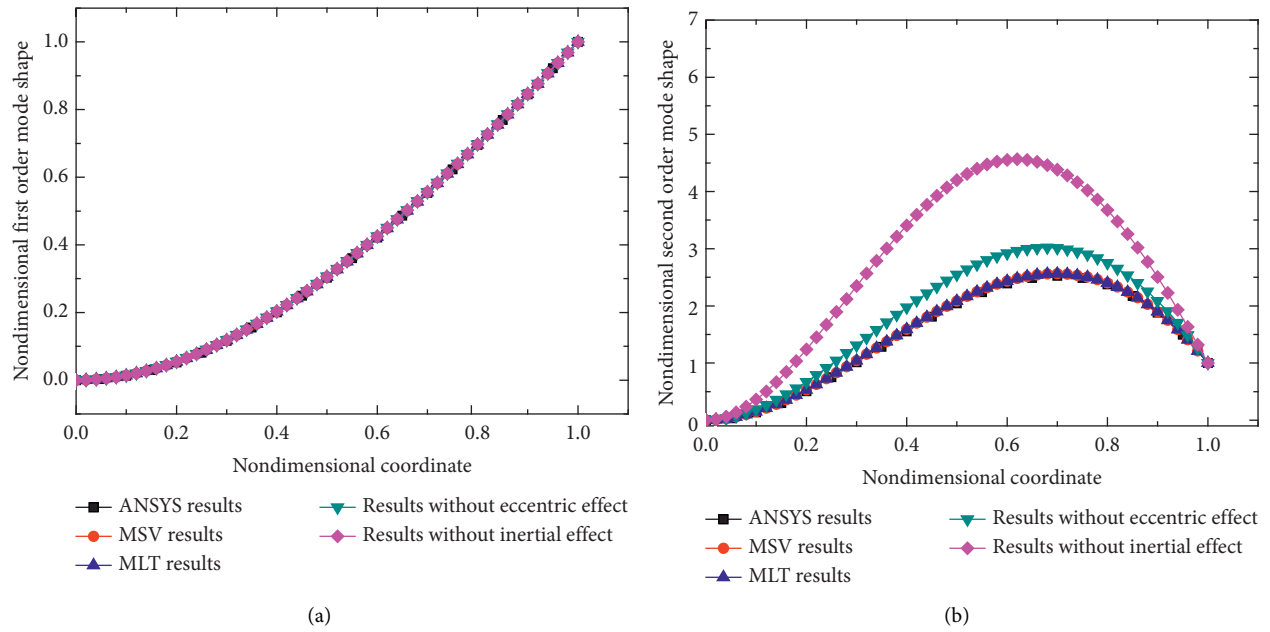

Figure 2: Continued.

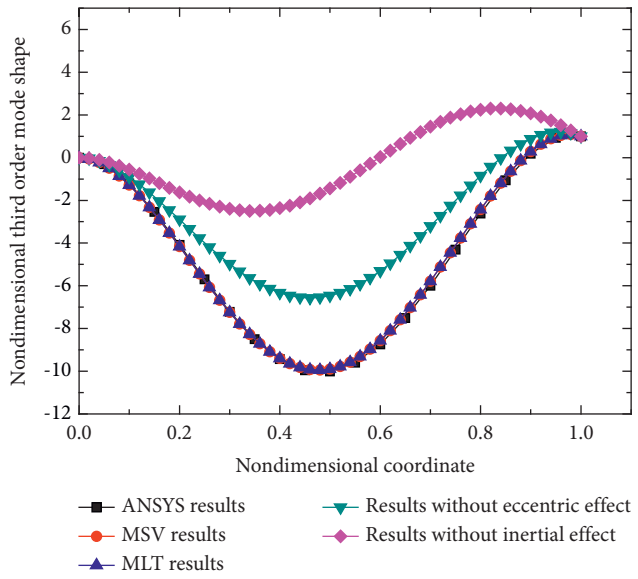

(c)

Figure 2: Comparisons of the mode shapes with the beam length of 100 mm. (a) The first-order mode shape. (b) The second-order mode shape. (c) The third-order mode shape.

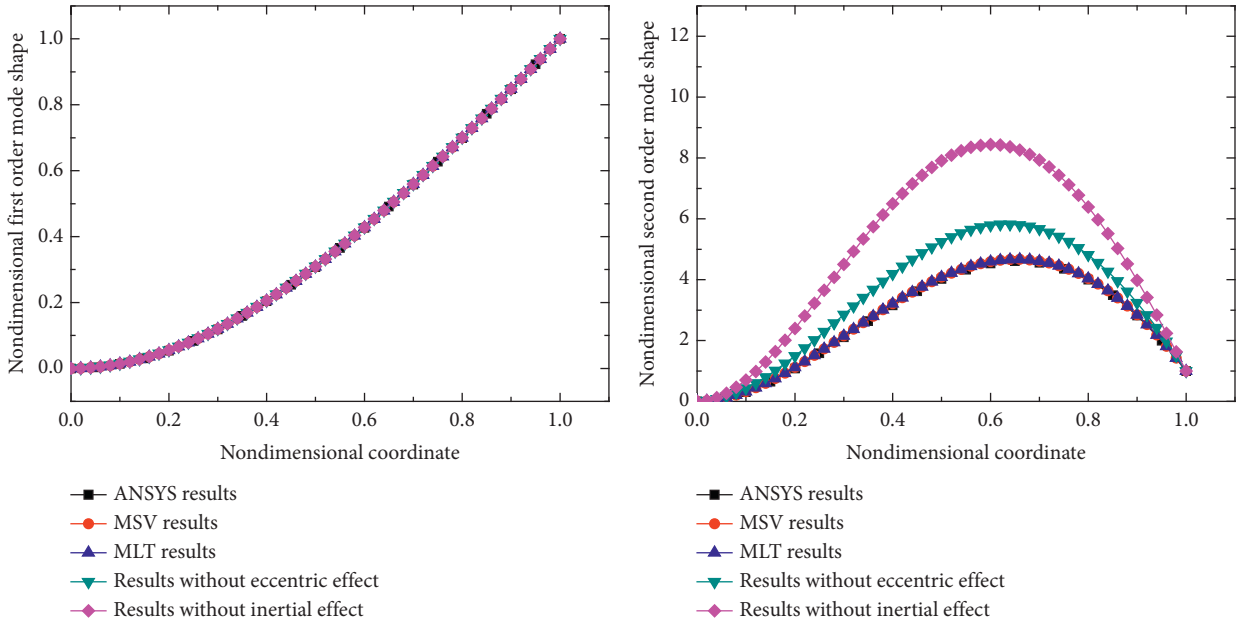

(a) (b)

Figure 3: Continued.

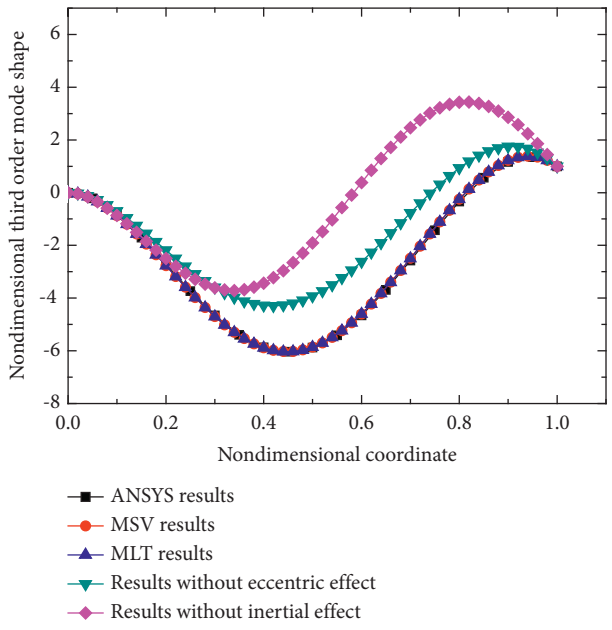

(c)

Figure 3: Comparisons of the mode shapes with the beam length of 150 mm. (a) The first-order mode shape. (b) The second-order mode shape. (c) The third-order mode shape.

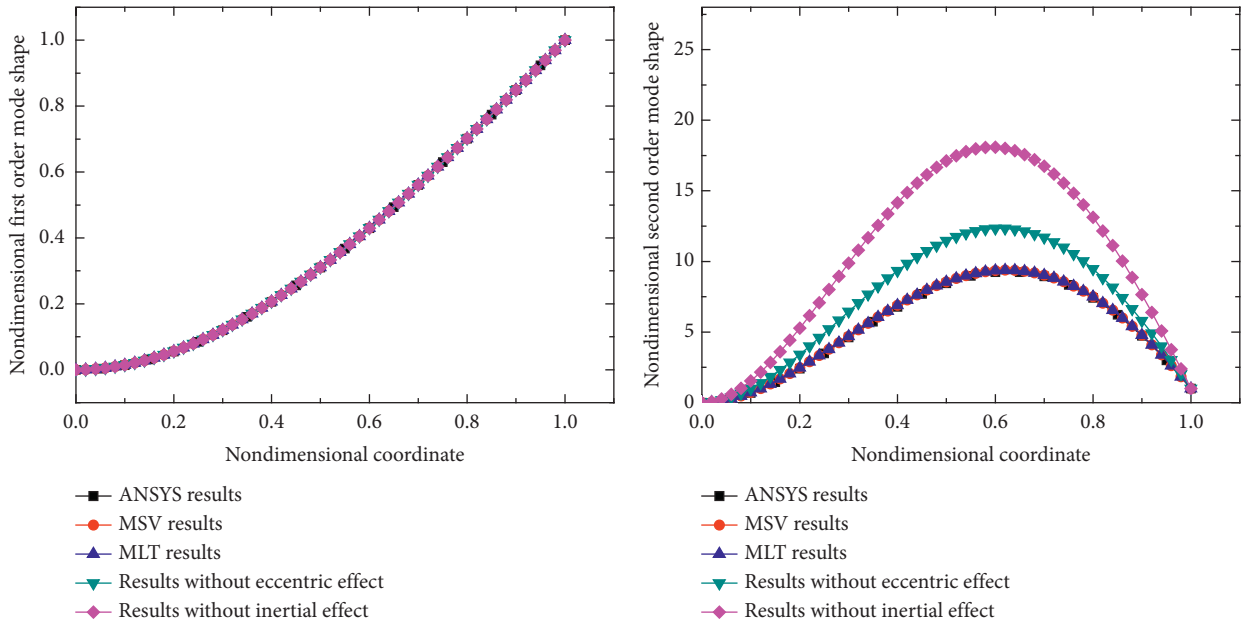

(a) (b)

Figure 4: Continued.

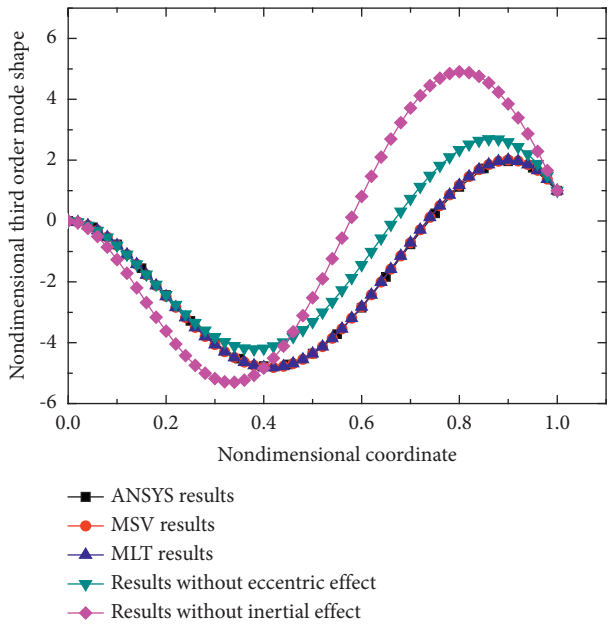

(c)

Figure 4: Comparisons of the mode shapes with the beam length of 200 mm. (a) The first-order mode shape. (b) The second-order mode shape. (c) The third-order mode shape.

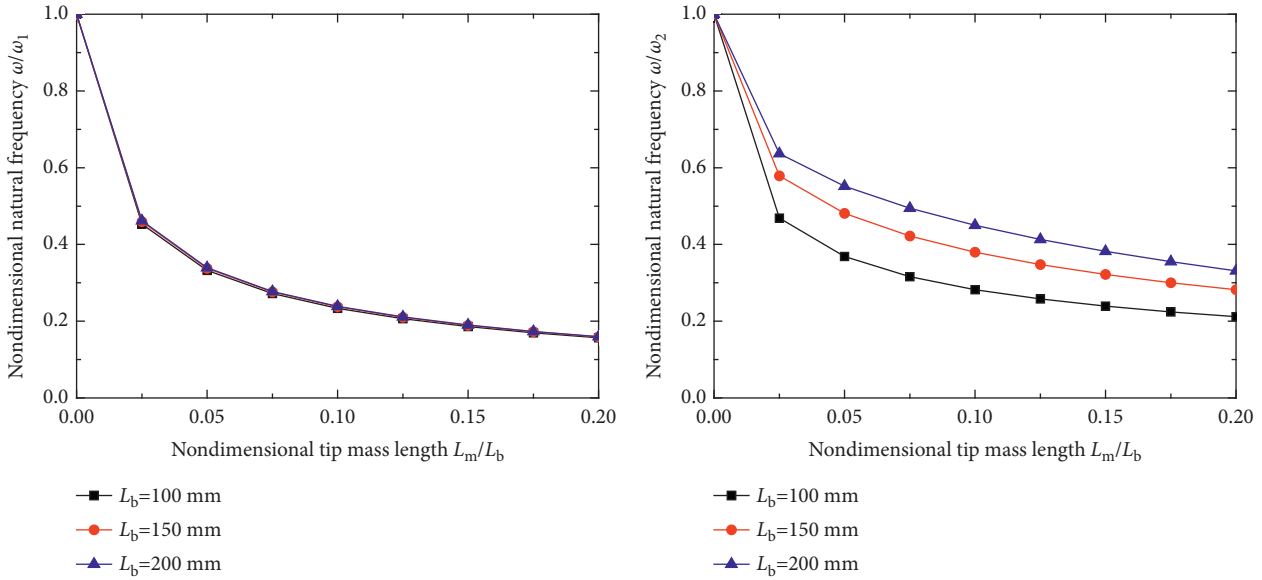

(a) (b)

Figure 5: Continued.

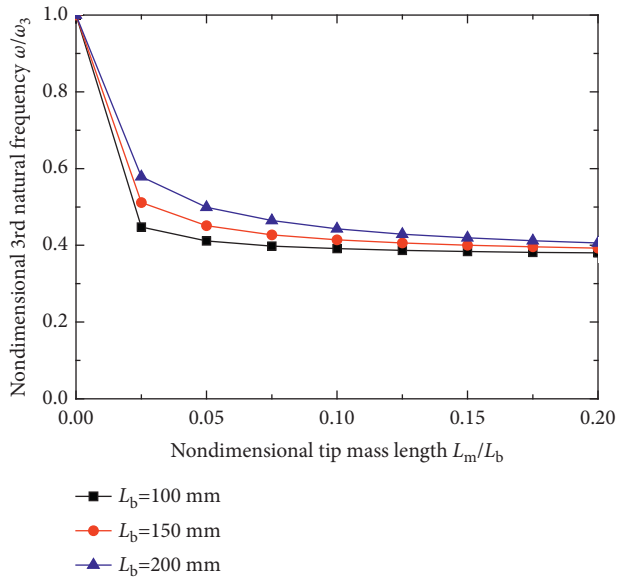

(c)

Figure 5: Variations of the nondimensionless natural frequencies with relative length of the tip mass to the beam. (a) The first-order natural frequency. (b) The second-order natural frequency. (c) The third-order natural frequency.

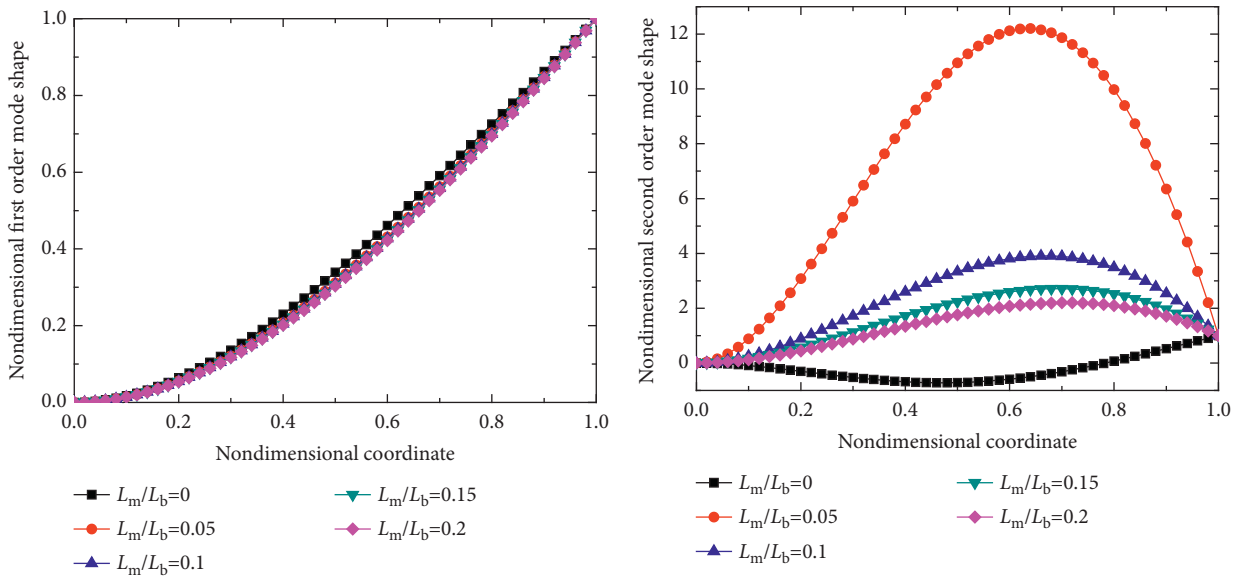

(a) (b)

Figure 6: Continued.

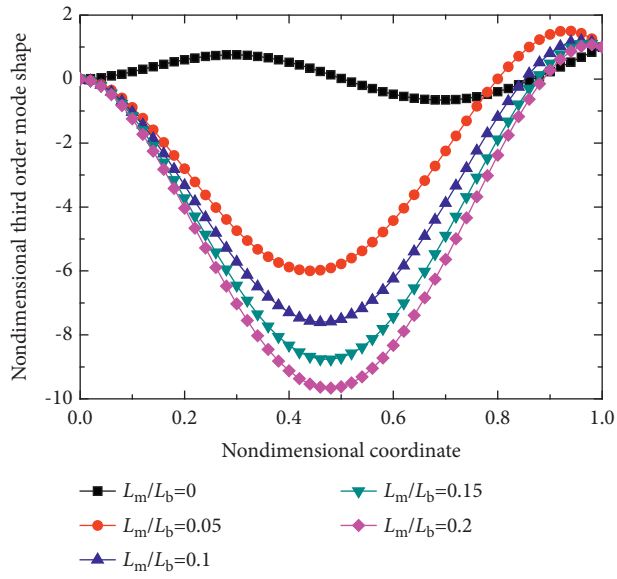

(c)

FIGURE 6: Variations of the nondimensionless mode shapes with relative length of the tip mass to the beam (L_b = 150 mm). (a) The first-order natural frequency. (b) The second-order natural frequency. (c) The third-order natural frequency.

and mode shapes obtained by MSV and MLT are exactly the same with each other. It is clear that the eccentric effect and inertial effect play an important role in the free vibration of the cantilever beam with an asymmetrically attached tip mass, and the quantitative investigations of some key parameters on the natural frequencies and mode shapes are given in the following section.

3.2. Parametric Investigations. The geometry and physical parameters of the basic structure used in the parametric investigations are given in Table 1, and the variations of the first three natural frequencies and corresponding mode shapes with relative length of the tip mass to the beam are given in Figures 5 and 6 , respectively. The mode shapes are normalized by the tip displacement, and the natural frequencies are normalized by ω_i (i = 1, 2, and 3) given below:

$$\omega_i = \left(\frac{\beta_i}{L_b}\right)^2 \sqrt{\frac{EI}{\rho_b A}}, \tag{61}$$

where β_1 = 1.875, β_2 = 4.694, and β_3 = 7.855.

It can be seen from Figure 5 that, with the increment of the relative length of the tip mass, all the first three orders of natural frequencies decrease due to the large tip mass effect. It is also noted that, for all the beams, the first- and third-order frequencies have the same tendency with respect to the nondimensionless tip mass length ratio, while for the second-order free vibration, the nondimensional natural frequency decreases from 1 to 0.21 with the increment of nondimensional tip mass length from 0 to 0.2 for the 100 mm length beam, while for the 150 mm and 200 mm beam, the nondimensional natural frequency decreases from 1 to 0.28 and 0.33, respectively. In other words, longer beam corresponds to smaller tip mass effect, and the frequency reduction phenomena with the increment of the tip mass length is more sensitive for the second-order natural frequency than the first-and third-order frequencies. Figure 6 shows the variations of the first three mode shapes of the 150 mm length beam with different nondimensionless tip mass length ratios, and it is very clear that, for the first-order free vibration, big tip mass can only reduce the natural frequency, while the first-order mode shape almost does not change. For higher-order mode shapes, the tip mass has more obvious effect, and the accurate mode shapes as well as the strain nodes are very important for higher-order vibration-based piezoelectric energy harvesting applications [25].

4. Conclusions

Free vibration analysis of a cantilever beam with an asymmetrically attached tip mass is performed. Both the traditional method of separation of variables (MSV) and the method of Laplace transform (MLT) are employed in the present paper, and the equivalent concentrate force and moment of the tip mass in the MLT are clarified. Numerical results show the accuracy of the present MSV and MLT, and the effect of the tip mass to the natural frequencies and corresponding mode shapes is also numerically investigated. Results show that tip mass has an obvious effect on the natural frequencies and mode shapes of the cantilever, other than the first-order mode shape. The present approach can also be used to solve beam structures with other boundary conditions and many concentrated mass locates at any position of the beam. It is also noted that it is easy for the Laplace transform method to obtain the orthogonality relations defined with respect to the variable density beam in the forced vibration analysis.

Data Availability

The data used to support the findings of the study are included within the article.

Conflicts of Interest

The authors declare that there are no conflicts of interest regarding the publication of this paper.

Acknowledgments

This work was supported by Guangdong Power Grid Corporation Science and Technology Project "Key Technology Based on Prefabricated Cabin Equipment of the Whole Substation" (037700KK52190022).

References

[1] S. Adhikari and S. Bhattacharya, "Dynamic analysis of wind turbine towers on flexible foundations," *Shock and Vibration*, vol. 19, no. 1, pp. 37–56, 2012.

[2] R. Bhat and M. A. Kulkarni, "Natural frequencies of a cantilever with slender tip mass," *AIAA Journal*, vol. 14, no. 4, pp. 536-537, 1976.

[3] B. Rama Bhat and H. Wagner, "Natural frequencies of a uniform cantilever with a tip mass slender in the axial direction," *Journal of Sound and Vibration*, vol. 45, no. 2, pp. 304–307, 1976.

[4] S. A. Mousavi Lajimi and G. R. Heppler, "Comments on "Natural frequencies of a uniform cantilever with a tip mass slender in the axial direction"," *Journal of Sound and Vibration*, vol. 331, no. 12, pp. 2964–2968, 2012.

[5] R. B. Bhat, "Authors' response to the comments on, "Natural frequencies of a uniform cantilever with a tip mass slender in the axial direction"," *Journal of Sound and Vibration*, vol. 331, no. 12, pp. 2962-2963, 2012.

[6] H. Wang, Q. Meng, and W. Feng, "Discussion of the improved methods for analyzing a cantilever beam carrying a tip-mass under base excitation," *Shock and Vibration*, vol. 2014, pp. 1–15, 2014.

[7] G. L. Anderson, "Natural frequencies of a cantilever with an asymmetrically attached tip mass," *AIAA Journal*, vol. 16, no. 3, pp. 281-282, 1978.

[8] C. W. S. To, "Vibration of a cantilever beam with a base excitation and tip mass," *Journal of Sound and Vibration*, vol. 83, no. 4, pp. 445–460, 1982.

[9] L. A. Parnell and M. H. Cobble, "Lateral displacements of a vibrating cantilever beam with a concentrated mass," *Journal of Sound and Vibration*, vol. 44, no. 4, pp. 499–511, 1976.

[10] C. A. Rossit and P. A. A. Laura, "Free vibrations of a cantilever beam with a spring-mass system attached to the free end," *Ocean Engineering*, vol. 28, no. 7, pp. 933–939, 2001.

[11] M. Gürgöze, "On the eigenfrequencies of a cantilever beam with attached tip mass and a spring-mass system," *Journal of Sound and Vibration*, vol. 190, no. 2, pp. 149–162, 1996.

[12] M. Gürgöze, "On the approximate determination of the fundamental frequency of a restrained cantilever beam carrying a tip heavy body," *Journal of Sound and Vibration*, vol. 105, no. 3, pp. 443–449, 1986.

[13] D. Zhou, "The vibrations of a cantilever beam carrying a heavy tip mass with elastic supports," *Journal of Sound and Vibration*, vol. 206, no. 2, pp. 275–279, 1997.

[14] M. N. Hamdan and B. A. Jubran, "Free and forced vibrations of a restrained uniform beam carrying an intermediate lumped mass and a rotary inertia," *Journal of Sound and Vibration*, vol. 150, no. 2, pp. 203–216, 1991.

[15] C. N. Bapat and C. Bapat, "Natural frequencies of a beam with non-classical boundary conditions and concentrated masses," *Journal of Sound and Vibration*, vol. 112, no. 1, pp. 177–182, 1987.

[16] J.-S. Wu and S.-H. Hsu, "A unified approach for the free vibration analysis of an elastically supported immersed uniform beam carrying an eccentric tip mass with rotary inertia," *Journal of Sound and Vibration*, vol. 291, no. 3-5, pp. 1122–1147, 2006.

[17] G. W. Morgan, "Some remarks on a class of eigenvalue problems with special boundary conditions," *Quarterly of Applied Mathematics*, vol. 11, no. 2, pp. 157–165, 1953.

[18] Y. Chen, "On the vibration of beams or rods carrying a concentrated mass," *Journal of Applied Mechanics*, vol. 30, no. 2, pp. 310-311, 1963.

[19] R. P. Geol, "Vibrations of a beam carrying a concentrated mass," *Journal of Applied Mechanics*, vol. 40, pp. 821-822, 1973.

[20] R. P. Goel, "Free vibrations of a beam-mass system with elastically restrained ends," *Journal of Sound and Vibration*, vol. 47, no. 1, pp. 9–14, 1976.

[21] W. H. Liu and C.-C. Huang, "Free vibration of restrained beam carrying concentrated masses," *Journal of Sound and Vibration*, vol. 123, no. 1, pp. 31–42, 1988.

[22] T.-P. Chang, "Forced vibration of a mass-loaded beam with a heavy tip body," *Journal of Sound and Vibration*, vol. 164, no. 3, pp. 471–484, 1993.

[23] S. Park, W. K. Chung, Y. Youm, and J. W. Lee, "Natural frequencies and ope-loop responses of an elastic beam fixed on a moving cart and carrying an intermediate lumped mass," *Journal of Sound and Vibration*, vol. 230, no. 3, pp. 591–615, 2000.

[24] W. Soedel, "On the philosophy of absolute truth in structural vibrations," *Journal of Sound and Vibration*, vol. 93, no. 3, pp. 465–468, 1984.

[25] A. Erturk, P. A. Tarazaga, J. R. Farmer, and D. J. Inman, "Effect of strain nodes and electrode configuration on piezoelectric energy harvesting from cantilevered beams," *Journal of Vibration and Acoustics*, vol. 131, pp. 11010-11011, 2009.